Design and Performance of a Monolithically Integrated Widely Tunable All-Optical Wavelength Converter With Independent Phase Control

Milan L. Mašanović, *Student Member, IEEE*, Vikrant Lal, *Student Member, IEEE*, Joseph A. Summers, *Student Member, IEEE*, Jonathon S. Barton, *Student Member, IEEE*, Erik J. Skogen, *Member, IEEE*, Larry A. Coldren, *Fellow, IEEE*, and Daniel J. Blumenthal, *Fellow, IEEE*

***Abstract*—We report on a new widely tunable all-optical wavelength converter consisting of a sampled-grating distributed Bragg reflector (SGDBR) laser monolithically integrated with a Mach–Zehnder interferometer semiconductor optical amplifier (MZI-SOA)-based wavelength converter. The new design incorporates independent phase control of the interferometer and SOAs for amplification of the SGDBR output. For the first time, error-free operation for data rates of up to 10 Gb/s is reported for 35-nm output tuning range. The high-speed operation is enabled by high photon density in the SOA due to large power transfer from the on-board tunable laser and amplifiers. We also report on device sensitivity of −10 dBm at 2.5 Gb/s and −5 dBm at 10 Gb/s, with an average output power of 0 dBm.**

***Index Terms*—Mach–Zehnder interferometer (MZI), photonic integrated circuits (PICs), tunable laser, wavelength conversion, wavelength converter.**

I. Introduction

FUTURE optical networks and their deployment represent the main driving force for the development of photonic integrated circuits (PICs). PICs utilize a single substrate for the monolithic integration of optically interconnected guided-wave optoelectronic devices. The primary objectives of photonic integration are similar to those of electronic integration: enhancing the performance, efficiency, reliability, and increasing the functionality while lowering the manufacturing and utilization cost. One of the key new PICs being developed for deployment in reconfigurable and packet-switched wavelength-division-multiplexing networks is the tunable all-optical wavelength converter (TAO-WC). Integration of the tunable laser and an all-optical Mach–Zehnder interferometer (MZI)-based wavelength converter on a single chip allows data to be transferred from an input wavelength to a tunable output wavelength without passing the signal through electronics. This class of wavelength converters was shown to work for both return-to-zero and non-return-to-zero (NRZ) data formats while acting as a 2R signal regenerator due to their highly nonlinear transfer function [1].

Manuscript received March 9, 2004; revised April 28, 2004. This work was supported by the DARPA/MTO CS-WDM Program under Grant N66001-02-C-8026.

The authors are with the Electrical and Computer Engineering Department, University of California Santa Barbara, Santa Barbara, CA 93106 USA (e-mail: mashan@ece.ucsb.edu).

Digital Object Identifier 10.1109/LPT.2004.834448

Previously, we have reported on the demonstration of the first widely TAO-WC [2]. With TAO-WC, we demonstrated regenerative, error-free operation at 2.5 Gb/s, with 22-nm output tuning range, −6-dBm input sensitivity, and −2 dBm in fiber converted signal power [3]. However, in this prior work, there were issues with optimization of the extinction ratio in the noninverting mode of operation, as well as the gain recovery time of the MZI semiconductor optical amplifiers (MZI-SOAs).

In this letter, we address these issues with a new device design. The major differences in the new design are the inclusion of an independent MZI-SOA interferometer phase control mechanism, and the addition of the two booster SOAs after the SGDBR laser. With this improved PIC design, we achieved error-free power efficient operation for bit rates up to 10 Gb/s, with increased output tuning range of 35 nm, and an increased input sensitivity and converted signal power.

II. Wavelength Converter Design

The new tunable wavelength converter design incorporates an SGDBR laser and a Mach–Zehnder SOA-based wavelength converter, but it differs from our previous design [2] in several key aspects: optimized sampled-grating DBR mirror design, two independent (for redundancy) longer input SOA, two booster-amplifier SOAs located in the branches of the MZI after the SGDBR laser, passive waveguide phase sections in the MZI, and finally, a dual-output multimode interference (MMI) 2×2 coupler at the wavelength converter output.

The electron micrograph of the chip on a carrier, as well as the wavelength converter schematic are shown in Fig. 1. The tunable SGDBR laser is 1.7 mm long and its operating principles are described in detail in [4]. The interferometer branches are defined by four S-bends and two 1.5-mm-long SOAs. The output light of the SGDBR laser is equally split using a 1×2 MMI-based light splitter, and then amplified by the two booster-amplifier SOAs that are located after the splitter, in the interferometer S-bends. This amplified laser light is then coupled with the light from the input waveguides using 2×1 MMI combiners into the SOAs in the branches of the MZI. The input signal is coupled onto the chip through a tapered, angled input waveguide, and then amplified by the input SOA running alongside the laser. In order to reduce the thermal crosstalk, the input SOAs, on the sides of the SGDBR laser, are about 200 μm away

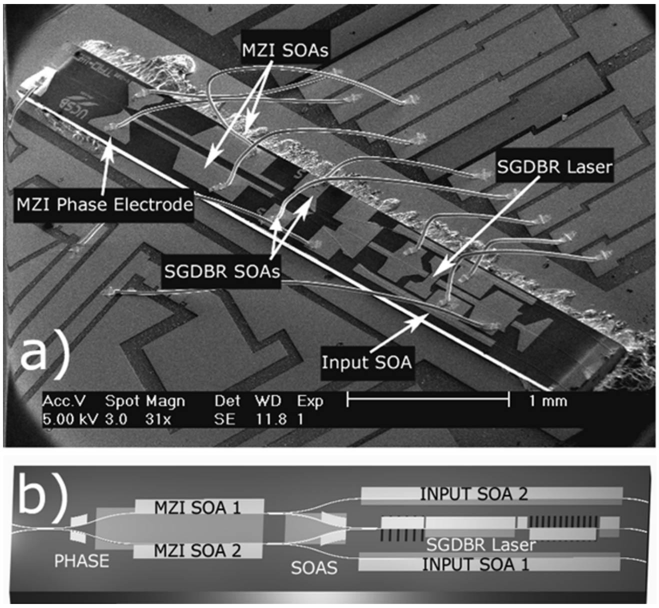

Fig. 1. (a) Electron micrograph of the wavelength converter. (b) Device schematic.

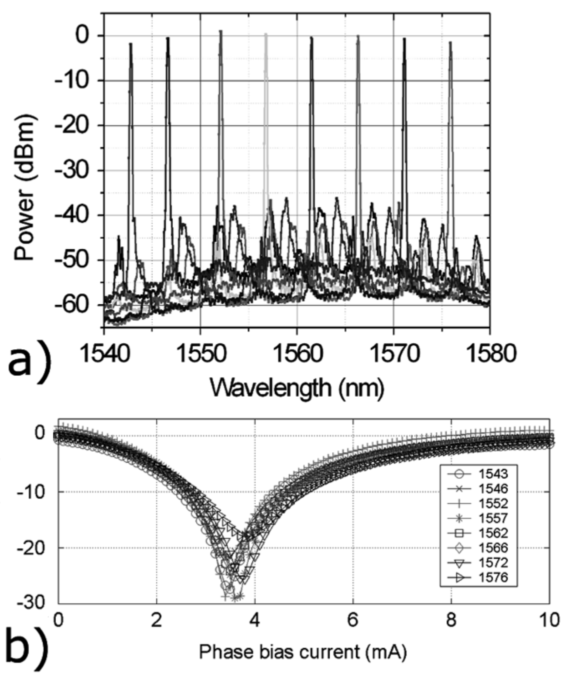

Fig. 2. (a) Spectra of the integrated laser. (b) Control of the interferometer using phase electrodes (Port 2: $I_{\mathrm{mzisoas}} = 200$ mA).

laterally from the SGDBR active region. The total chip size is 0.5×5.3 mm.

The laser mirror design was optimized for wide tunability, resulting in 35-nm output tuning range [see Fig. 2(a)].

Longer input SOA helps improve the device sensitivity by providing a large amount of gain, as seen in Fig. 3(b). The total gain shown represents the gain measured at the input to the left MZI-SOA, and therefore, includes the propagation loss of the signal through the passive waveguides and light splitters. The power measurements on chip for both Fig. 3(a) and (b) were

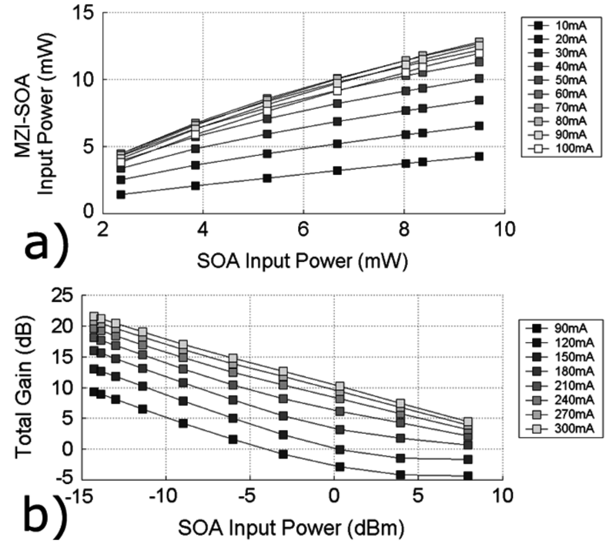

Fig. 3. (a) Power of the SGDBR-generated light that reaches the MZI-SOA as a function of the booster amplifier bias current. (b) Gain of the preamplifier SOA measured at the MZI-SOA.

performed by reverse biasing the SOAs and measuring the photocurrent.

Two 250-μm-long SOAs are used to amplify the continuous-wave (CW) light from the SGDBR laser. These amplifiers provide about 5 dB of gain resulting in more than 12 mW of optical power entering each MZI-SOAs. This high-power optical pumping sets the MZI-SOAs in the high-photon density operation regime, thereby reducing the gain recovery time to less than 60 ps and enabling 10-Gb/s operation. The gain recovery time was measured from the optical eye diagram. Measured SGDBR light power in the MZI-SOAs in function of the SGDBR output power is shown in Fig. 3(a).

For independent adjustment of the SOA gain in the MZI and the relative phase between the two branches, two phase control sections consisting of 100-μm-long passive waveguides were incorporated into this design. The effect used to achieve the index change is carrier plasma effect, which is observed when a diode is in forward bias and the carriers are flowing through the waveguide. This method of phase control is fairly wavelength insensitive, as shown in Fig. 2(b). We observe better than 25 dB of extinction over 30-nm range. The measurements show absolute power coupled and were taken without an output filter, therefore, we notice a degradation in the extinction observed for wavelengths more than 20 nm away from the gain peak due to reduced amplified spontaneous emission (ASE) suppression at those wavelengths. This separation of phase control provides for easier optimization of the operating bias point of the wavelength converter as well as better extinction for both inverting and noninverting modes of operation, in part because the gain of the MZI-SOA can be adjusted to compensate for high ASE light power of the input amplifier in the OFF state of the wavelength converter.

The branches of the MZI are joined by an MMI-based 2×2 coupler at the output. Depending on the relative phase of the CW light in the MZI branches, the total light power will be distributed between the two output waveguides with two extreme cases: For the phase difference of $-90°$, all of the light will be coming out of one waveguide, whereas, for the phase difference of $+90°$, all of the light will be coming out of the other waveguide. This output scheme is useful because it allows for the CW light to be continuously removed from the chip (this is different from our previous design [2]), which helps with light evacuation from the chip. Both of the output waveguides are curved and tapered before they reach the facet in order to minimize the back reflections [3].

The device was fabricated using an offset quantum-well integration platform and process, and the details about the process have been reported in [3]. For this work, we used a lower loss $1.4Q$ quaternary waveguide.

III. Device Performance

Device characterization was performed using two lensed fibers to couple light into and out of the device. Tuning results of the on-chip laser are shown in Fig. 2(a)—device tuning range is 35 nm with better than 35-dB side-mode suppression ratio.

The relative phase of the two branches is adjusted using the phase electrodes to cancel out the CW signals. As can be seen from Fig. 2(b), less than 4 mA is required to turn the interferometer off completely; therefore, the new method of phase control is very efficient.

For wavelength conversion, a transverse-electric polarized input signal at 1570 nm was generated using an electrooptic modulator with NRZ $2^{31}-1$ pseudorandom bit sequence data at both 2.5 and 10 Gb/s. The converted output wavelength was filtered using a thin-film tunable filter and detected with a PIN-photodiode-based receiver. The MZI SOA biases were set to cancel out the preamplifier ASE influence. Measured bit-error-rate (BER) curves are shown in Fig. 4. The signal input power to the device was -10 dBm for 2.5-Gb/s operation and -5 dBm for 10-Gb/s operation. The bias currents were kept constant for all wavelength. The average output power of the wavelength converter was 0 dBm. At 2.5 Gb/s, the maximum power penalty measured was 0.8 dB which can be attributed mainly to the ASE noise generated by the on-chip SOAs. At 10 Gb/s, the power penalty was measured as low as 1.4 dB for output wavelengths between 1542–1555 nm. The penalty increased to around 3 dB, and the BER slope decreased for longer wavelengths (above 1570 nm), which can be attributed to different SNR redistribution due to optical transfer function change for wavelengths near the band edge. The dynamic extinction ratios were better than 10 dB for both bit rates.

IV. Conclusion

Design and performance of a new monolithically integrated widely tunable all-optical wavelength converter in InP were reported in this letter. This new design allowed for both simple optimization of the device operating point and superior performance relative to our previous work [2]. Error-free operation for data rates up to 10 Gb/s over 35-nm output tuning range of the device was demonstrated for the first time for a monolithically integrated tunable wavelength converter. The device input sensitivity for error-free operation was -10 dBm at 2.5 Gb/s and -5 dBm at 10 Gb/s. The average converted signal output power of the device was 0 dBm.

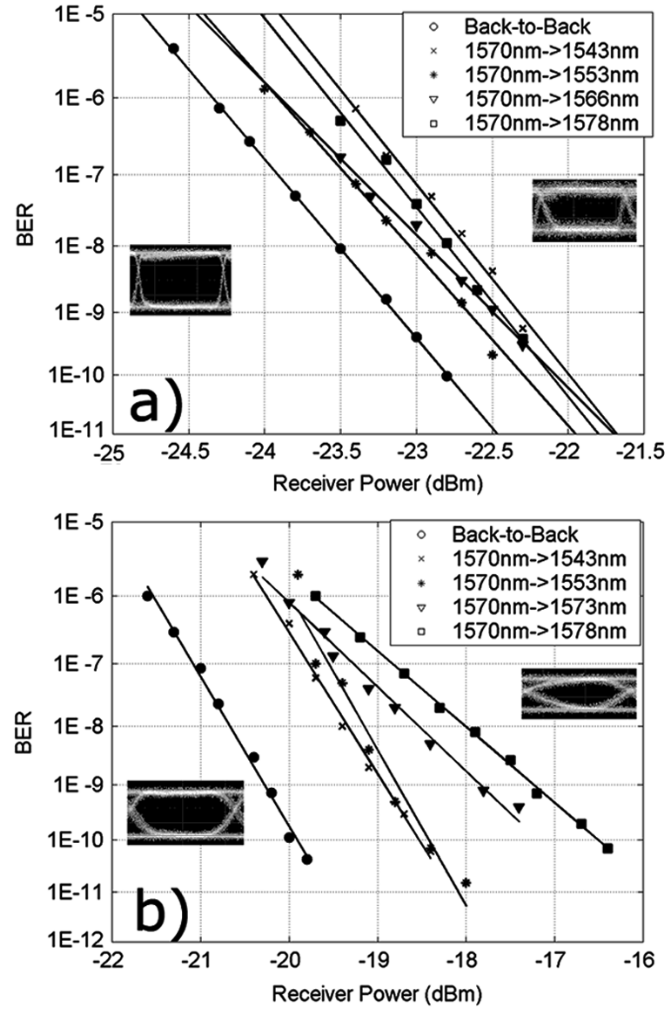

Fig. 4. (a) BER testing results for operation at 2.5 Gb/s. (b) BER testing results for operation at 10 Gb/s. The device bias currents were $I_{\rm gain}=93$ mA, $I_{\rm mzisoa-left}=300$ mA, $I_{\rm mzisoa-right}=265$ mA, $I_{\rm input}=200$ mA, $I_{\rm booster}=45$ mA.

Acknowledgment

The authors would like to thank Agility Communications for MOCVD growth and AR coating services, and Marcelo Davanço from UCSB for help with the FE-SEM.

References

[1] D. Wolfson, T. Fjelde, A. Kloch, C. Janz, F. Poingt, F. Pommereau, I. Guillemot, F. Gaborit, and M. Renaud, "Detailed experimental investigation of all-active dual-order mode Mach-Zehnder wavelength converter," *Electron. Lett.*, vol. 36, pp. 1296–1297, 2000.

[2] M. L. Mašanović, V. Lal, J. S. Barton, E. J. Skogen, L. A. Coldren, and D. J. Blumenthal, "Monolithically integrated Mach-Zehnder interferometer wavelength converter and widely-tunable laser in InP," *IEEE Photon. Technol. Lett.*, vol. 15, no. 8, pp. 1117–1119, Aug. 2003.

[3] M. L. Mašanović, V. Lal, J. A. Summers, J. S. Barton, E. J. Skogen, L. G. Rau, L. A. Coldren, and D. J. Blumenthal, "Widely-tunable monolithically-integrated all-optical wavelength converters in InP," *J. Lightwave Technol.*, submitted for publication.

[4] V. Jayaraman, Z. Chuang, and L. Coldren, "Theory, design, and performance of extended tuning range semiconductor lasers with sampled gratings," *IEEE J. Quantum Electron.*, vol. 29, pp. 1824–1834, June 1993.